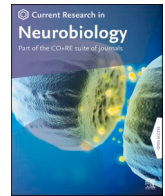




Contents lists available at ScienceDirect

Current Research in Neurobiology

journal homepage: www.sciencedirect.com/journal/current-research-in-neurobiology

Thalamic nuclei changes in early and late onset Alzheimer's disease

Gonzalo Forno^{a,b,c,2}, Manojkumar Saranathan^{d,2}, Jose Contador^a, Nuria Guillen^a,
 Neus Falgàs^{a,e}, Adrià Tort-Merino^a, Mircea Balasa^{a,e}, Raquel Sanchez-Valle^{a,f},
 Michael Hornberger^{g,1}, Albert Lladó^{a,f,1,*}

^a Alzheimer's Disease and Other Cognitive Disorders Unit, Neurology Service, Hospital Clínic of Barcelona, Institut d'Investigacions Biomèdiques August Pi i Sunyer (IDIBAPS), Barcelona, Spain

^b Laboratorio de Neuropsicología y Neurociencias Clínicas (LANNEC), Facultad de Medicina, Universidad de Chile, Chile

^c School of Psychology, Universidad de los Andes, Santiago, Chile

^d Radiology, University of Massachusetts Chan Medical School, Worcester, MA, United States

^e Atlantic Fellow for Equity in Brain Health, Global Brain Health Institute, University of California San Francisco, Trinity College Dublin, Ireland

^f Institute of Neurosciences, Department of Medicine, Faculty of Medicine and Health Sciences, University of Barcelona, Barcelona, Spain

^g Norwich Medical School, University of East Anglia, Norwich, UK

ARTICLE INFO

Keywords:

Thalamus
 Thalamic nuclei
 Early onset Alzheimer's disease
 Late onset Alzheimer's disease
 THOMAS-DL

ABSTRACT

Alzheimer's disease (AD) is the most common cause of dementia worldwide. Increasing evidence points to the thalamus as an important hub in the clinical symptomatology of the disease, with the 'limbic thalamus' been described as especially vulnerable. In this work, we examined thalamic atrophy in early-onset AD (EOAD) and late-onset AD (LOAD) compared to young and old healthy controls (YHC and OHC, respectively) using a recently developed cutting-edge thalamic nuclei segmentation method. A deep learning variant of Thalamus Optimized Multi Atlas Segmentation (THOMAS) was used to parcellate 11 thalamic nuclei per hemisphere from T1-weighted MRI in 88 biomarker-confirmed AD patients (49 EOAD and 39 LOAD) and 58 healthy controls (41 YHC and 17 OHC) with normal AD biomarkers. Nuclei volumes were compared among groups using MANCOVA. Further, Pearson's correlation coefficient was computed between thalamic nuclear volume and cortical—subcortical regions, CSF tau levels, and neuropsychological scores. The results showed widespread thalamic nuclei atrophy in EOAD and LOAD compared to their respective healthy control groups, with EOAD showing additional atrophy in the centromedian and ventral lateral posterior nuclei compared to YHC. In EOAD, increased thalamic nuclei atrophy was associated with posterior parietal atrophy and worse visuospatial abilities, while LOAD thalamic nuclei atrophy was preferentially associated with medial temporal atrophy and worse episodic memory and executive function. Our findings suggest that thalamic nuclei may be differentially affected in AD according to the age at symptoms onset, associated with specific cortical—subcortical regions, CSF total tau and cognition.

1. Introduction

Alzheimer's disease (AD) is the most prevalent cause of dementia worldwide and is often characterized as a 'hippocampal dementia' (Craig et al., 2011), i.e. the main initial pathology is focused around the hippocampus and neighbouring medial temporal lobe regions. This prevailing view might be, however, misleading since it is known for

decades that other structures of the Papez circuit are also affected by AD pathophysiology at the same time as the hippocampus (Braak, 1991). It is well known that the Papez circuit, comprised of the hippocampus, fornix, mammillary bodies (MB), anterior thalamic nuclei (ATN), posterior cingulate cortex (PCC), and parahippocampal cortex (PHC) (Papez, 1937), is highly sensitive to AD pathophysiology, as well as its clinical symptomatology (e.g., Hornberger et al., 2012, for a review see (Forno

* Corresponding author. Alzheimer's disease and other cognitive disorders unit, Neurology Service, Hospital Clínic, IDIBAPS, Universitat de Barcelona, C/Vil·larroel, 170, Barcelona, 08036, Spain.

E-mail address: allado@clinic.cat (A. Lladó).

¹ These authors share senior authorship.

² These authors share co-first authorship.

<https://doi.org/10.1016/j.crneur.2023.100084>

Received 17 January 2023; Received in revised form 27 February 2023; Accepted 14 March 2023

Available online 24 March 2023

2665-945X/© 2023 The Authors. Published by Elsevier B.V. This is an open access article under the CC BY-NC-ND license (<http://creativecommons.org/licenses/by-nc-nd/4.0/>).

et al., 2021)).

Among the Papez circuit structures, the thalamus is gaining attention. Increasing evidence confirms the earlier neuropathological findings that the thalamus is a crucial hub in the clinical symptomatology of the disease, with the anterior, laterodorsal, and the mediodorsal thalamic nuclei ('limbic thalamus') (Taber et al., 2004) especially vulnerable to AD (Aggleton et al., 2016). This dovetails with Braak and Braak's seminal paper (Braak and Braak, 1991), showing neurofibrillary tau tangles in the anterodorsal thalamic nuclei at the same time as the hippocampus. However, until recently most human studies were confined to neuropathological studies, since in vivo neuroimaging of patients only allowed investigation of the whole thalamus and not specific thalamic nuclei due to technical shortcomings. Fortunately, recent methodological advances have made it possible to use standard imaging sequences (i.e., MPRAGE) for the investigation of thalamic nuclei. Indeed, studies have started to report thalamic nuclei changes in prodromal and symptomatic AD with biomarker confirmation (Bernstein et al., 2021; Iglesias et al., 2018; Low et al., 2019). The results seem largely to confirm neuropathological findings and therefore offer an opportunity to understand how Papez circuit structures outside of the medial temporal lobe contribute to the disease onset, progression, and symptomatology of AD.

To our knowledge, all of the AD thalamic nuclei investigations have focused on the late-onset variant of AD, with only one study analysing subregional thalamic changes in a cohort of young *presenilin 1* carrier (Pardilla-Delgado et al., 2021). Late-onset AD (LOAD) is clinically defined as people presenting with AD after the age of 65, whereas early-onset AD (EOAD) is defined as those presenting with AD before the age of 65. Although 65 is an arbitrary age threshold for the definition, intriguing differences have been described between EOAD and LOAD, with younger age associated with a faster progressive variant of AD (Mendez, 2012; Tort-Merino et al., 2022), increased frequency of atypical AD and different distribution of AD pathophysiology. Higher prevalence of primarily visuospatial, language, and behavioural/dysexecutive impairment (i.e., non-amnesic) are found in EOAD compared to LOAD (Koedam et al., 2010). EOAD also shows a higher burden of neurofibrillary tangles (NFT) in neocortical regions, while more affected medial temporal lobe areas are in LOAD (Murray et al., 2011; Scholl et al., 2017). Further, EOAD shows a greater density of senile plaques (Ho et al., 2002) and greater neuronal loss (Koedam et al., 2010) overall. LOAD is more associated with medial temporal lobe changes than EOAD, while EOAD presents greater frontoparietal or temporoparietal atrophy. Specifically, a significant decrease in volume in the occipital, parietal, and frontal lobes have been found in EOAD compared to LOAD, whereas reduced left hippocampal volume found the opposite contrast (Frisoni et al., 2007). Similar results have been described in longitudinal analysis, as EOAD at 3 years follow-up presents with increased cortical thinning in the left frontoparietal and left superior temporal cortex, left cingulate gyri, bilateral posterior cingulate, and precuneus compared to LOAD. The opposite contrast showed more rapid cortical thinning on the left parahippocampal gyrus in LOAD compared to EOAD (Cho et al., 2013). To our knowledge, it is not clear whether thalamic nuclei are also differentially affected by the age of onset of the disease.

The current study addresses this gap by investigating thalamic nuclei atrophy in EOAD and LOAD patients compared to age-matched young and old healthy control subjects (YHC and OHC, respectively). Importantly, we use a recently developed cutting-edge deep learning based thalamic segmentation method, which has been shown to allow more reliable thalamic nuclei segmentation compared to existing methods. We further analysed the relationship of specific thalamic nuclei and the corresponding cortical atrophy. Finally, we investigated how the thalamic nuclei atrophy in EOAD and LOAD relates to tau CSF levels and their cognitive symptomatology.

2. Methods

2.1. Participants

Fifty EOAD and 42 LOAD patients were recruited from the Alzheimer's disease and Other Cognitive Disorders Unit at the Hospital Clinic de Barcelona (HCB), Barcelona, Spain. Each participant underwent neurological and neuropsychological assessments, 3T brain MRI, and a spinal tap for CSF biomarkers. All of them met the NIA-AA diagnostic criteria for Mild Cognitive Impairment (MCI) due to AD, or mild dementia due to AD presenting the core cerebrospinal fluid (CSF) biomarkers levels suggesting the presence of AD neuropathology (A + T+) with neurodegeneration (N+) (Jack et al., 2018; McKhann et al., 2011). These 92 patients were complemented by 41 young healthy controls (YHC) and 18 old HC (OHC), with normal CSF AD biomarkers levels and normal cognition. Participants with prior mental illness, head trauma, cerebrovascular disease, or alcohol and drug abuse were excluded. After visual inspection, 1 LOAD and 1 EOAD participants were removed due to failed MRI thalamic nuclei segmentation. We then removed participants that had 5 or more nuclei above or below 3 standard deviations from their own sample mean nuclear volumes. The final sample comprised of 49 EOAD, 39 LOAD, 41 YHC, and 17 OHC cases. Of the 49 EOAD, 2 presented with primary visuospatial impairment (posterior cortical atrophy [PCA]) and 1 with language impairment (logopenic variant of primary progressive aphasia [PPA]). We did not include any participant with an autosomal dominant pattern (ADAD) caused by a mutation in *presenilin 1*, *presenilin 2*, or amyloid precursor protein. No participant presented with primary motor symptoms.

Ethics approval for this study was obtained from the HCB Ethics Committee. All the participants provided informed consent in accordance with the Declaration of Helsinki.

2.2. Cerebrospinal fluid biomarkers

Baseline CSF sample was obtained from all the participants. Levels of amyloid- β ($A\beta_{42}$) (until June 2019), phosphorylated tau (p-tau), and total-tau (t-tau), were analysed using commercially available single-analyte enzyme-linked immunosorbent assay (ELISA) (INNOTEST, FUJIREBIO Europe N.V., Gent, Belgium). $A\beta_{42}$ levels from collected samples since July 2019 were analysed using Lumipulse (FUJIREBIO Europe N.V., Gent, Belgium). Cut-off values for CSF $A\beta_{42}$ (A), p-tau (T), and t-tau (N) were determined following internal cut-off (Antonell et al., 2020).

2.3. Imaging acquisition

All imaging was performed in a 3T Magnetom Trio Tim scanner (Siemens Medical Systems, Germany) at the Magnetic Resonance Imaging Core Facility. Whole-brain high-resolution T1-weighted MPRAGE anatomical 3D spin echo volumes, parallel to the plane connecting the anterior and posterior commissures was used to generate 240 contiguous slices with the following parameters: repetition time (TR) = 2300 ms; echo time (TE) = 2,98 ms; Field-of-view (FOV) = 256 mm; matrix dimension = 256 \times 256; section thickness = 1 mm, voxel size = 1 \times 1 \times 1 mm³).

2.4. Data processing

Thalamic nuclei parcellation was carried out using a recently proposed deep learning variant of the THOMAS (Thalamus optimized multi-atlas segmentation (Su et al., 2019)), technique. We refer to this method henceforth as THOMAS-DL, which is described in detail in (Umapathy et al., 2021). Briefly, THOMAS-DL comprises of two concatenated convolutional neural networks (CNN)- the first takes as input standard T1 images and synthesizes white-matter (WM) nulled MPRAGE images, where WM is nulled instead of cerebrospinal fluid as in conventional T1

MRI. This significantly improves the definition of the whole thalamic boundary as well as intra-thalamic nuclear contrast and has shown to outperform standard THOMAS for conventional T1 MRI (Umapathy et al., 2021). The synthesized WMn MPRAGE images are then segmented using another CNN which was trained using THOMAS segmentation data on cases where both WMn and T1 images were acquired and registered. The use of CNN-based segmentation eliminated the need for image registration used in THOMAS, which is time consuming and can be challenging in patients with enlarged ventricles. Both CNNs were 2.5D U-nets which achieved a compromise between memory requirements and ability to use through-plane information (Fig. 1). Each thalamus was segmented into 11 nuclei (anteroventral nucleus [AV], ventral anterior nucleus [VA], ventral lateral anterior nucleus [VLA], ventral lateral posterior nucleus [VLP], ventral posterior lateral nucleus [VPL], Pulvinar nucleus, lateral geniculate nucleus [LGN], medial geniculate nucleus [MGN], centromedian nucleus [CM], mediodorsal nucleus [MD], habenula [Hb]) and the mammillothalamic tract [MTT].

The segmented labels were then used to estimate left and right thalamic nuclei volumes (L,R) and a laterality index (Low et al., 2019) calculated for each nucleus as follows:

$$LI = (L-R) / (0.5 * (L + R)) * 100\%$$

Resulted volumes were combined in order to obtain each thalamic nucleus volume.

We also estimated the volume of 5 ROIs -hippocampus, entorhinal cortex, PCC, precuneus, and PHC- using Freesurfer v6.0.0 (<https://surfer.nmr.mgh.harvard.edu/>). Detailed Freesurfer preprocessing steps are fully reported elsewhere (Dale et al., 1999; Fischl and Dale, 2000). Total intracranial volumes (TIV) were calculated for each participant from the output Freesurfer's *recon-all* command. All volumes (i.e. thalamic nuclear and Freesurfer ROIs) were adjusted for TIV and age using the residual method (Pintzka et al., 2015). Briefly, the adjusted volumes were calculated by computing a regression slope between YHC and OHC volumes and TIVs. The resulting slope was then used for the calculation of adjusted volumes using the following formula:

$$Vol_{adj} = Vol - b * (TIV - \overline{TIV})$$

where Vol_{adj} is the TIV adjusted volume, Vol is the original unadjusted volume, b is the slope from the linear regression of Vol on TIV , and \overline{TIV} the mean TIV (Pintzka et al., 2015). We then repeated the same procedure on the TIV adjusted volumes using age instead of TIV to obtain TIV and age adjusted volumes. The formula was calculated separately for YHC and OHC. TIV and age adjusted volumes were used for the Pearson's correlation calculations.

2.5. Statistical analysis

Continuous variables were checked for normality using Shapiro-Wilk test. Biological sex was analysed using chi-squared test (χ^2). Age and

education differences were analysed using one-way ANOVAs. Disease duration (time from the age at symptom onset until the cognitive assessment) was compared between EOAD and LOAD using independent-sample *t*-test. Then we analysed cognitive and CSF data using a one-way ANOVA for EOAD vs YHC. As significant differences in age were found between LOAD and OHC, we ran a one-way MANCOVA with age as covariate of interest. This analysis was then repeated when comparing EOAD and LOAD.

Thalamic nuclei and the 5 ROI volumes selected were further analysed. Each thalamic nucleus was compared in three different contrasts. EOAD and LOAD were compared to their respective control group and between themselves using three one-way MANCOVA tests with age and TIV as covariates of interest. The procedure was also repeated for the 5 Freesurfer ROIs. Then, we wanted to understand how thalamic nuclei are associated with specific cortical and subcortical structures. For this, thalamic nuclei most commonly associated with the Papez circuit (AV, VA, Pulvinar and MD nucleus) were selected and Pearson's correlation coefficient computed. The 5 ROIs adjusted volumes were selected as dependent variables and the TIV—age adjusted thalamic nuclei as independent variables. These analyses were run separately for EOAD and LOAD.

Then, we repeated this procedure with CSF p-tau and t-tau levels. In this case, we selected all 11 TIV—age thalamic nuclei as independent variable and performed Pearson's correlation with each CSF marker as a dependent variable. We excluded $A\beta_{42}$ levels for the correlation analyses as $A\beta_{42}$ levels were analysed with different methodologies over time and results might be non-comparable. Only AD patients were used for correlation calculations (i.e. healthy controls subjects were not used).

Finally, we analysed the contribution of the 4 previously selected thalamic nuclei to cognitive performance in EOAD and LOAD. For these, we extended the analysis with each neuropsychological test/variable as dependent variable and TIV—age adjusted thalamic nuclei volumes as independent variable.

The cognitive variables selected were the MMSE (Folstein and McHugh, 1975) for global cognition, four measures of the Free and Cued Selective Reminding Test (FCSRT) (Grober et al., 1988) including the free recall ([FCSRT_FR, the number of words recall after the three trials with no cued provide], the total immediate recall ([FCSRT_TIR, the sum of the free recall items and the cued recall items across the three trials]), the differ free recall ([FCSRT_DFR, the freely recall words after 20 min delay]), and the total differ recall ([FCSRT_TDR, the sum of the spontaneously item recall and the cued items after 20 min) for episodic memory, semantic and phonemic fluency (Casals-Coll et al., 2013) for executive function, as well as the Trail Making Test B and Trail Making Test A (TMT B and A) (Tamayo et al., 2012) also assessing attention and Visual Object and Space Perception (VOSP) letters and numbers (Warrington and James, 1991) for visuospatial abilities. Again, correlations were run separately for EOAD and LOAD using an exploratory approach.

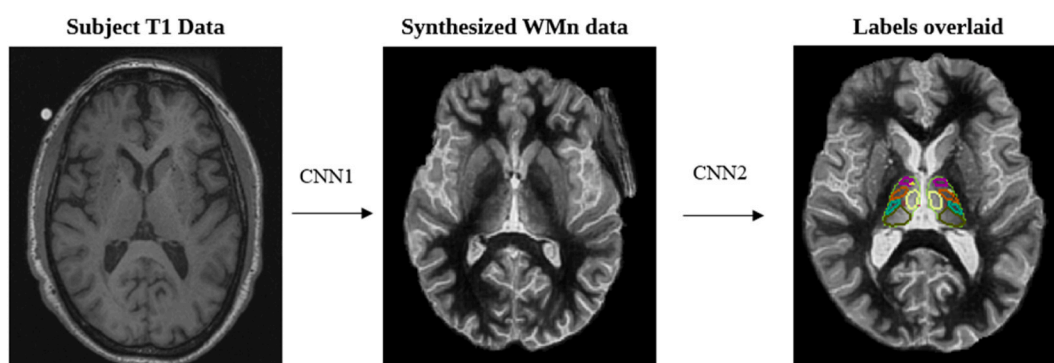


Fig. 1. Thalamic nuclei segmentation using THOMAS-DL.

3. Results

3.1. Descriptive results

No differences in age or education were found between EOAD and YHC. LOAD were significantly older than EOAD and OHC, but no differences in years of education were found among them. EOAD had longer disease duration compared to LOAD. EOAD performed significantly worse than YHC in all cognitive assessments. Compared to OHC, LOAD had poorer results in global cognition, episodic memory, semantic fluency and executive function with preserved phonemic fluency and visuospatial abilities. Although no significant differences were found in cognition between EOAD and LOAD, a trend toward significance was found in general cognition (MMSE; $p = 0.082$) and attention (TMT A; $p = 0.055$) with EOAD showing worse performance than LOAD. For CSF tau, both EOAD and LOAD showed altered p-tau and t-tau values compared to their respective controls. No significant differences were found between EOAD and LOAD in CSF tau levels (Table 1).

3.2. Thalamic volume atrophy

Compared to their respective groups, both EOAD and LOAD revealed significantly decreased volume in the AV nucleus ($p \leq 0.01$, $d = 0.65$; $p \leq 0.05$, $d = 0.60$, respectively), VA nucleus ($p \leq 0.001$, $d = 1.18$; $p \leq 0.05$, $d = 0.88$, respectively), VLa nucleus ($p \leq 0.01$, $d = 0.54$; $p \leq 0.01$, $d = 0.93$, respectively), VPL nucleus ($p \leq 0.001$, $d = 0.80$; $p \leq 0.001$, $d = 1.19$, respectively), Pulvinar nucleus ($p \leq 0.001$, $d = 1.08$; $p \leq 0.05$, $d = 1.14$, respectively) and MD nucleus ($p \leq 0.001$, $d = 0.94$; $p \leq 0.01$, $d = 1.15$, respectively). No significant differences were found in LGN, MGN and Hb in EOAD and LOAD. In addition, EOAD also showed a significant volume decrease in VLP ($p \leq 0.001$, $d = 0.84$) and CM nucleus ($p \leq 0.001$, $d = 0.82$). There were no significant differences when comparing thalamic nuclei volumes between EOAD and LOAD (Fig. 2). Laterality index showing thalamic nuclei atrophy are detailed in the supplementary material. Briefly, lateralized index resembled thalamic volume results with specific differences. When comparing EOAD to YHC, VLa atrophy was left lateralized and significant left Hb volume was also found in EOAD. For LOAD and OHC, AV volume decreased was only found in the right AV nucleus, and decreased VLP and LGN volume were left lateralized in LOAD (see supplementary material).

3.3. Cortical volume atrophy

Compared to YHC, EOAD presents widespread atrophy as a significant volume decrease was found in the entorhinal cortex ($p \leq 0.001$, $d = 0.94$), hippocampus ($p \leq 0.001$, $d = 1.48$), PCC ($p \leq 0.003$, $d = 0.67$), precuneus ($p \leq 0.001$, $d = 1.05$) and PHC ($p \leq 0.001$, $d = 0.72$). LOAD pattern of volume loss compared to OHC, was restricted to the medial temporal lobe, with significant atrophy in the entorhinal cortex ($p \leq 0.05$, $d = 0.68$), the hippocampus ($p \leq 0.001$, $d = 1.73$) and the PHC ($p \leq 0.01$, $d = 0.92$). No significant results were found when comparing EOAD and LOAD.

3.4. Thalamic correlations

3.4.1. Cortical-thalamic regions

Both EOAD and LOAD showed positive cortical—thalamic correlations. EOAD showed the following correlations [AV nucleus—PCC ($p \leq 0.05$, $r = 0.33$); AV nucleus—Precuneus ($p \leq 0.05$, $r = 0.31$); VA nucleus—PCC ($p \leq 0.05$, $r = 0.29$); Pulvinar nucleus—PCC ($p \leq 0.001$, $r = 0.48$); Pulvinar—Precuneus ($p \leq 0.05$, $r = 0.3$); Pulvinar nucleus—PHC ($p \leq 0.05$, $r = 0.3$); MD nucleus—PCC ($p \leq 0.05$, $r = 0.29$)], while LOAD cortical—thalamic correlations were [AV nucleus—entorhinal ($p \leq 0.05$, $r = 0.33$); AV nucleus—hippocampus ($p \leq 0.05$, $r = 0.34$); VA nucleus—hippocampus ($p \leq 0.05$, $r = 0.37$); Pulvinar nucleus—Entorhinal ($p \leq 0.05$, $r = 0.32$); Pulvinar

Table 1

Descriptive results.

	YHC (n = 41)	OHC (n = 17)	EOAD (n = 49)	LOAD (n = 39)
Age	59.94 (4.1)	70.48 (4.63)	60.1 (4.3)	74.45 ^{††} (4.61)
Gender (M:F)	10:31	5:12	22:27	19:20
Education	11.27 (4.07)	10.88 (9.81)	10.36 (4.7)	9.81 (4.15)
Disease Duration (years)	–	–	3.15 [†] (1.84)	2.14 (1.76)
MMSE	28.66 (1.65)	27.58 (1.44)	22.5 ^{***} (3.58)	25.93 [†] (3.11)
FCSRT_FR (Maximum Score of 48)	27.5 (6.11)	23.08 (10.62)	9.16 ^{***} (7.41)	12.29 ^{†††} (7.82)
FCSRT_TFR (Maximum Score of 48)	42.68 (4.47)	42.08 (4.44)	22.19 ^{***} (14.12)	24.84 ^{†††} (14.95)
FCSRT_DFR (Maximum Score of 16)	10.35 (1.96)	9.42 (2.11)	3.38 ^{***} (4.03)	2.94 ^{†††} (3.54)
FCSRT_TDR (Maximum Score of 16)	14.8 (1.24)	14.5 (1.45)	6.99 ^{***} (6.11)	8.12 ^{†††} (5.55)
Semantic Fluency	22.03 (5.67)	20.17 (5.47)	11.81 ^{***} (4.86)	15.89 [†] (5.64)
Phonemic Fluency	35.71 (12.55)	33.42 (10.72)	24.54 ^{***} (13.29)	28.07 (14.83)
TMT A	39.82 (24.84)	50.33 (15.95)	98.5 ^{***} (52.49)	57.53 (34.13)
TMT B	100.27 (55.52)	102.92 (37.59)	250.79 ^{***} (77.56)	207.05 ^{†††} (73.09)
VOPS Letters	19.6 (0.6)	19.67 (0.65)	17.93 ^{***} (2.98)	19.3 (1.97)
VOSP Numbers	9.13 (0.94)	9.58 (0.52)	7.03 ^{***} (2.98)	8.55 (1.97)
CSF Aβ ₄₂ ‡ (Before June 2019)	830.76 (224.64)	757.65 (181.53)	398.6 (125.24)	342.74 (88.07)
CSF Aβ ₄₂ ‡ (Since June 2019)	–	–	492.73 (144.57)	359.78 (106.52)
CSF t-Tau	206.73 (56.58)	244.82 (124.17)	831.12 ^{***} (454.91)	894.79 ^{†††} (479.53)
CSF p-Tau	47.34 (10.19)	52.02 (15.49)	119.94 ^{***} (71.29)	122.99 ^{†††} (42.51)

Note. Data are presented in mean (standard deviation). * $p \leq 0.05$; ** $p \leq 0.01$; *** $p \leq 0.001$ for the comparison between YHC and EOAD; † $p \leq 0.05$; †† $p \leq 0.01$; ††† $p \leq 0.001$ for the comparison between OHC and LOAD; Abbreviation YHC: Young healthy controls; OHC: Old healthy controls; EOAD: Early onset Alzheimer's disease; LOAD: Late onset Alzheimer's Disease; MMSE: Mini-Mental State Exam; FCSRT_FR: FCSRT Free Recall; FCSRT_TFR: FCSRT Total Free Recall; FCSRT_DFR: FCSRT Defer Free Recall; FCSRT_TDR: FCSRT Total Defer Recall; † $p \leq 0.05$ comparison between EOAD and LOAD; ‡ CSF Aβ₄₂ values are provided with a diagnostic value only.

Missing data for Education: 2 EOAD, 2 LOAD.

Missing data for MMSE: 3 EOAD, 2 LOAD.

Missing data for FCSRT_FR: 1 YHC, 1 OHC, 11 EOAD, 5 LOAD.

Missing data for FCSRT_TFR: 1 YHC, 1 OHC, 11 EOAD, 6 LOAD.

Missing data for FCSRT_DFR: 1 YHC, 1 OHC, 11 EOAD, 6 LOAD.

Missing data for FCSRT_TDR: 1 YHC, 1 OHC, 11 EOAD, 6 LOAD.

Missing data for Semantic Fluency: 1 YHC, 8 EOAD, 2 LOAD.

Missing data for Phonemic Fluency: 3 YHC, 1 OHC, 13 EOAD, 3 LOAD.

Missing data for TMT A: 2 YHC, 10 EOAD, 2 LOAD.

Missing data for TMT B: 7 YHC, 4 OHC, 29 EOAD, 11 LOAD.

Missing data for VOSP Letters: 7 YHC, 10 EOAD, 2 LOAD.

Missing data for VOSP Numbers: 1 YHC, 2 OHC, 12 EOAD, 3 LOAD.

nucleus—hippocampus ($p \leq 0.001$, $r = 0.49$); Pulvinar nucleus—PCC ($p \leq 0.001$, $r = 0.49$); Pulvinar—Precuneus ($p \leq 0.01$, $r = 0.43$); Pulvinar nucleus—PHC ($p \leq 0.05$, $r = 0.36$); MD nucleus—PCC ($p \leq 0.01$, $r = 0.43$).

3.4.2. Thalamus and CSF biomarkers

EOAD AV nucleus was negatively associated with t-tau ($p \leq 0.05$, $r =$

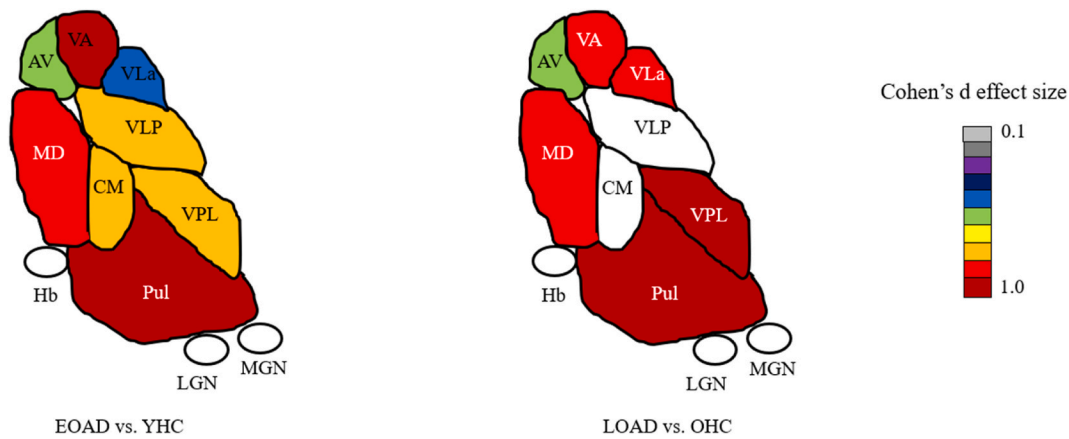


Fig. 2. Thalamic nuclei atrophy for EOAD and LOAD compared to YHC and OHC respectively, colored by effect size (only statistically significant atrophy is shown).

-0.31), while LOAD showed no significant associations between thalamic nuclei and tau.

3.4.3. Thalamus and neuropsychology

A significant association between the AV nucleus and visuospatial abilities (VOPS letters ($p \leq 0.05, r = 0.36$) and numbers ($p \leq 0.05, r = 0.34$)) was found in EOAD. For LOAD, the AV nucleus correlated with episodic memory (FCSRT_TIR ($p \leq 0.05, r = 0.37$); FCSRT_TDR ($p \leq 0.05, r = 0.38$)). The VA, Pulvinar and MD nuclei significantly correlated with semantic fluency ($p \leq 0.05, r = 0.35$); ($p \leq 0.01, r = 0.56$); ($p \leq 0.01, r = 0.43$) respectively). The Pulvinar nucleus was also significantly associated with phonemic fluency ($p \leq 0.01, r = 0.49$) (Fig. 3).

4. Discussion

In this study, we analysed the volume changes of different thalamic nuclei across EOAD and LOAD. We further investigated how these changes are related with cortical atrophy, CSF tau levels and association with cognitive impairment. Overall, widespread thalamic nuclei atrophy was observed in EOAD when compared to YHC, as well as for LOAD and OHC. While preserved LGN, MGN and Hb was found in EOAD, it showed additional atrophy in VLP and CM compared to LOAD.

The differences between LOAD and EOAD are intriguing since a DTI study described preferential tracts between the CM nucleus and sub-cortical regions, such as the hippocampus (Eckert et al., 2012).

Further, EOAD showed decreased attention compared to YHC, with no similar result when comparing LOAD to OHC. Notably, attention has been associated with CM integrity (Ilyas et al., 2019) and with increasing vulnerability in younger age at symptom onset (Smits et al., 2012). Within the ventral thalamic subnuclei, evidence showing smaller volume in AD is somehow inconsistent, likely due to poor thalamic boundary contrast in standard T1 which will lead to poor ventral nuclei volume estimation. While the few studies that have analysed specific thalamic nuclei integrity in AD described ventral shrinkage, the extent of ‘how much’ and which specific ventral nucleus is a matter of ongoing debate (Bernstein et al., 2021; Iglesias et al., 2018; Low et al., 2019). More consistent is the evidence showing increased AV nucleus atrophy (Bernstein et al., 2021; Iglesias et al., 2018; Low et al., 2019), which in this case was found in both EOAD and LOAD. This is not surprising as the AV is one of the so-called ‘limbic-thalamus’ which is highly interconnected with regions typically associated with AD and especially vulnerable to neurodegenerative disease (Aggleton, 2012; Aggleton et al., 2016; Hornberger et al., 2012). The AV nucleus has also been described as critical in the clinical symptomatology of the early prodromal stages of AD (Aggleton et al., 2016; Swartz and Black, 2006), which has been reinforced in recent imaging studies (Bernstein et al., 2021; Low et al., 2019). Moreover, AV nucleus shrinkage has been associated as a function of increasing cognitive impairment (Bernstein et al., 2021). Our results are in line with previous studies and come to reinforce the notion that the AV nucleus is critical in AD.

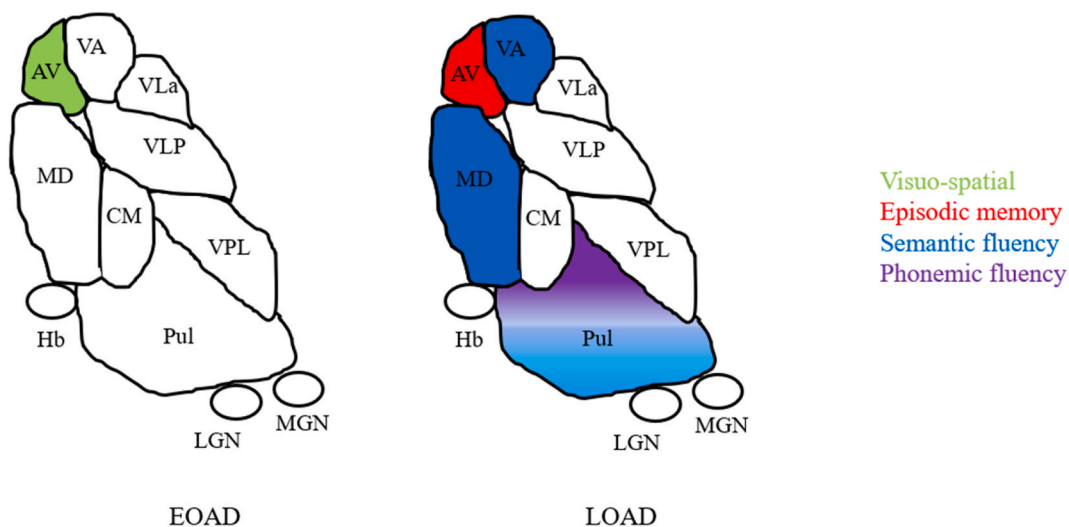


Fig. 3. Significant correlations between thalamic nuclei volumes and neuropsychological test scores. Note: Pulvinar volumes are correlated with both semantic and phonemic fluency.

Other than the AV nucleus, the MD and Pulvinar nuclei were significantly smaller in EOAD and LOAD. These nuclei are considered as ‘higher-order’ thalamic nuclei (Parnaudeau et al., 2018), and are associated with memory or memory-related regions, attention, and executive function (Homman-Ludiye and Bourne, 2019; Parnaudeau et al., 2018) and establish broad connections within the cortex (Eckert et al., 2012; Homman-Ludiye and Bourne, 2019; Parnaudeau et al., 2018). Changes in the MD nucleus have been described in a variety of conditions, such as Frontotemporal dementia (Bocchetta et al., 2020), Down’s Syndrome (Perry et al., 2019), and Parkinson’s disease (PD) (Thomas et al., 2020). Also, molecular changes in the Pulvinar nucleus have been described in Dementia with Lewy Bodies (DLB) which are hypothesized to contribute to cognitive symptomatology typically associated with DLB (Erskine et al., 2018). Overall, our results contribute to the consistent evidence showing changes in the MD and Pulvinar nucleus alongside different neurological disorders.

We were unable to replicate previous findings showing decreased volume in MGN (Bernstein et al., 2021; Iglesias et al., 2018) and LGN (Iglesias et al., 2018) in AD. Our null results could be explained by a methodology issue when segmenting LGN and MGN due to their smaller size and smaller sample size (order of magnitude) in our study compared to these studies. Further, a recent study has hypothesized that actual LGN/MGN atrophy could be explained due to visual or auditory input loss or account for a false positive (Iglesias et al., 2018). If LGN and MGN are indeed affected due to AD, it should be studied more carefully in future studies. Further, reduced volumes in ventral nuclei (VA, VL_a, VPL) were also found in EOAD and LOAD. As mentioned earlier, smaller VLP were also found in EOAD. A recent study showed increased atrophy in the left VA thalamic volume in AD patients, but no differences in global VA nucleus (Low et al., 2019). When looking at lateralized differences, our results showed bilateral VA atrophy in both EOAD and LOAD when compared with their respective healthy controls. Moreover, significant left but not right VL_a atrophy and bilateral VLP atrophy were found in EOAD when compared to YHC. For LOAD, bilateral VL_a atrophy and left but not right VLP atrophy were found when compared to OHC (see supplementary material). Although subtle differences in nuclei atrophy patterns appear in EOAD and LOAD, it seems that the left thalamic nucleus is more vulnerable to AD neuropathology. A previous study also showed a significant volume decrease in VLP and VA nucleus, but non-significant results in the VL_a and VPL nucleus (Bernstein et al., 2021). Although there is inconsistency in how specific ventral thalamic nuclei are affected by AD, it seems clear that the ventral thalamic region is somehow affected by AD and these warrant future studies.

Our thalamo—cortical correlation analyses showed significant associations for EOAD and LOAD. For EOAD, the AV, VA, Pulvinar and MD nucleus showed an important association with posterior parietal regions. Also, the Pulvinar nucleus was weakly associated with the PHC. It seems that the classical topographic pattern of GM volume loss in EOAD (Frisoni et al., 2005, 2007), may also affect how these structures are connected to specific thalamic nuclei. The Pulvinar—parahippocampal cortex correlations are in line with evidence showing abnormal connectivity in the default mode network (DMN) in PCA, which is more commonly associated with younger age at symptom onset (Schott and Crutch, 2019). Also, a longitudinal study showed changes in the parahippocampal cortex that were not detected at the time of diagnosis (Contador et al., 2021), which could indicate disease severity. Similar cortical—thalamic correlations were found for the Pulvinar and the MD nucleus in LOAD. Most notably, only LOAD AV, Pulvinar and VA nucleus correlated with the hippocampus and no significant AV—posterior cingulate correlations were found in LOAD. It seems that nuclei involved in cognition (i.e., AV and Pulvinar nucleus) are selectively correlated with structures typically associated with AD according to their age at symptom onset. This could suggest that age at symptom onset affects not only the vulnerability of selective cortical regions, but also how these regions relate to specific thalamic nuclei.

While EOAD showed significant negative correlation between AV

nucleus and t-tau, LOAD thalamic nuclei showed no significant association with tau levels. Neuropathological studies have described neurofibrillary changes in early stages of AD, specifically located in the anterodorsal thalamic nucleus (Stage III) with NFT present in the whole brain in the end stage (Braak and Braak, 1991). Distribution of tau pathology also differ between EOAD and LOAD, with younger patients more prone to tau aggregation in neocortical regions, whereas older patients more localized in medial temporal lobe (Scholl et al., 2017). Our results are in line with the hypothesis that age at symptom onset is related to more neurodegeneration and accelerated disease progress (Samgard et al., 2010).

When analysing thalamic—cognitive correlations, we found significant results for the AV, VA, Pulvinar and MD nuclei. Specifically, in EOAD, the AV nucleus showed important correlations with visuospatial abilities. Animal models have shown that navigation capacity could be mediated by head direction cells in the AV and its interaction with other cortical structures (Coughlan et al., 2018). To our knowledge, no studies on humans have addressed this issue properly. Although our results have to be taken with caution, this could be a starting point for the role that AV plays in visuospatial abilities in EOAD patients. In LOAD, the AV nucleus was significantly associated with episodic memory, which is in line with the hypothesis that this nucleus plays an important role in episodic memory (Aggleton, 2012; Aggleton et al., 2010, 2016; Bernstein et al., 2021), forming part of an integrated mnemonic circuit called, the Papez circuit (for a review see (Forno et al., 2021)). Our findings indicate that the AV nucleus could have a differential role in cognition according to the age at symptom onset. This is also supported, by our thalamic—cortical correlations, as EOAD AV nucleus was significantly associated with areas critical for normal visuospatial abilities (i.e., posterior parietal regions), while LOAD AV correlated with crucial areas for episodic memory (i.e., the hippocampus).

Also, the VA, MD and Pulvinar nuclei correlated with semantic fluency, while phonemic fluency was exclusively associated with the Pulvinar nucleus in LOAD. Our results align with previous studies showing a significant role of VA nucleus in verbal fluency (Low et al., 2019). Importantly, we demonstrated significant association with semantic but not verbal fluency, while Low and collaborators obtained verbal fluency sub-score from the Addenbrooke’s Cognitive Examination—Revised (ACE-R), which combines both verbal and semantic fluency in one score. Further, the MD nucleus has shown meaningful bilateral connections to the prefrontal cortex and the anterior cingulate cortex (Eckert et al., 2012), regions strongly associated with executive function (Carter et al., 1999; Friedman and Robbins, 2022). The Pulvinar nucleus is important for executive function (Ouhaz et al., 2018), which have already been described as a factor that may contribute to dysexecutive function in other dementias (Tak et al., 2020). This is in line with our results, as changes in the MD and the Pulvinar nucleus were associated with decreased cognitive flexibility. Also, a study conducted in PCA showed an important role of the Pulvinar nucleus in compensating non-visuospatial cognitive function by mediating cortical regions associated to the salience and DMN (Fredericks et al., 2019).

This study comes with limitations. We used a CNN-based method for thalamic segmentation. While this has been shown to improve accuracy compared to THOMAS in patients with alcohol use disorder, its sensitivity to specific nuclei still needs careful evaluation. Structures such as the LGN and MGN are not clearly discerned in T1 contrast and can pose issues for accurate segmentation. While the WMn synthesis approach deals with some of these issues, it can still be suboptimal. Future work could use directly acquired WMn MPRAGE data to further improve the accuracy of thalamic nuclei parcellation of small structures. Also, our thalamic—cortical correlation findings must be taken cautiously. Although our results are in line with structural and functional studies addressing thalamic—cortical projections, this needs to be further studied. Also, due to the small number of older healthy control, the contrast between LOAD and OHC may be biased. Lastly, this was a cross-sectional rather than a longitudinal study. A longitudinal study

examining conversion rates could prove very useful in elucidating imaging-based biomarkers.

5. Conclusions

In conclusion, this paper address structural thalamic nuclei changes in EOAD and LOAD, and how these changes are related to cognition, cortical regions and CSF biomarkers tau levels. We believe we provide novel and striking evidence on how thalamic nuclei are distinctly affected according to the age at symptom onset. Broadly, CM and VLP structural changes were exclusively found in EOAD. Most strikingly, AV changes in EOAD were associated with visuospatial impairment and levels of t-tau, while LOAD AV changes were related to episodic memory impairment and no thalamic nuclei associated to tau levels.

CRedit authorship contribution statement

Gonzalo Forno: contributed in, Conceptualization, Methodology, Formal analysis, Investigation, Visualization, Writing – original draft, and, Writing – review & editing. **Manojkumar Saranathan:** contributed in, Conceptualization, Methodology, Software, Validation, Investigation, Visualization, Writing – original draft, and, Writing – review & editing. **Jose Contador:** contributed in, Resources, Writing – review & editing. **Nuria Guillen:** contributed in, Resources, Writing – review & editing. **Neus Falgàs:** contributed in, Resources, Writing – review & editing. **Adrià Tort-Merino:** contributed in, Resources, Writing – review & editing. **Mircea Balasa:** contributed in, Resources, Writing – review & editing. **Raquel Sanchez-Valle:** contributed in, Resources, Writing – review & editing. **Michael Hornberger:** contributed in, Conceptualization, Methodology, Validation, Formal analysis, Investigation, Visualization, Writing – original draft, and, Writing – review & editing, Supervision, Project administration. **Albert Lladó:** contributed in, Conceptualization, Methodology, Validation, Formal analysis, Investigation, Visualization, Writing – original draft, and, Writing – review & editing, Supervision, Project administration.

Declaration of competing interest

The authors declare the following financial interests/personal relationships which may be considered as potential competing interests: Albert Lladó reports financial support was provided by Carlos III Health Institute. Mircea Balasa reports financial support was provided by Carlos III Health Institute. Michael Hornberger reports financial support was provided by Alzheimer's Research UK, Wellcome Trust. Neus Falgàs reports financial support was provided by Carlos III Health Institute. Nuria Guillen reports financial support was provided by Carlos III Health Institute.

Data availability

The data that has been used is confidential.

Acknowledgement

The authors thank patients, their relatives and healthy controls for their participation in the research. This work was supported by Instituto de Salud Carlos III (ISCIII) through the project PI19/00449 to Dr. A. Lladó, PI19/00198 to Dr M. Balasa and co-funded by the European Union and CERCA Programme/Generalitat de Catalunya. MH is funded by the Alzheimer's Research UK, Wellcome Trust, Medical Research Council and BBSRC. NF received funding by ISCIII Joan Rodes grant JR22/00014. NG received funding by ISCIII PFIS grant (FI20/00076).

Appendix A. Supplementary data

Supplementary data to this article can be found online at <https://doi.org/10.1016/j.crneur.2023.100084>.

References

- Aug Aggleton, J.P., 2012. Multiple anatomical systems embedded within the primate medial temporal lobe: implications for hippocampal function. *Neurosci. Biobehav. Rev.* 36 (7), 1579–1596. <https://doi.org/10.1016/j.neubiorev.2011.09.005>.
- Aggleton, J.P., O'Mara, S.M., Vann, S.D., Wright, N.F., Tsanov, M., Erichsen, J.T., 2010. Hippocampal-anterior thalamic pathways for memory: uncovering a network of direct and indirect actions. *Eur. J. Neurosci.* 31, 2292–2307. <https://doi.org/10.1111/j.1460-9568.2010.07251.x>.
- Jul Aggleton, J.P., Pralus, A., Nelson, A.J., Hornberger, M., 2016. Thalamic pathology and memory loss in early Alzheimer's disease: moving the focus from the medial temporal lobe to Papez circuit. *Brain* 139 (Pt 7), 1877–1890. <https://doi.org/10.1093/brain/aww083>.
- Feb Antonell, A., Tort-Merino, A., Rios, J., Balasa, M., Borrego-Ecija, S., Auge, J.M., Munoz-García, C., Bosch, B., Falgas, N., Rami, L., Ramos-Campoy, O., Blennow, K., Zetterberg, H., Molinuevo, J.L., Llado, A., Sanchez-Valle, R., 2020. Synaptic, axonal damage and inflammatory cerebrospinal fluid biomarkers in neurodegenerative dementias. *Alzheimers Dement* 16 (2), 262–272. <https://doi.org/10.1016/j.jalz.2019.09.001>.
- Bernstein, A.S., Rapcsak, S.Z., Hornberger, M., Saranathan, M., Alzheimer's Disease Neuroimaging, I., 2021. Structural changes in thalamic nuclei across prodromal and clinical Alzheimer's disease. *J Alzheimers Dis* 82 (1), 361–371. <https://doi.org/10.3233/JAD-201583>.
- Mar Bocchetta, M., Iglesias, J.E., Neason, M., Cash, D.M., Warren, J.D., Rohrer, J.D., 2020. Thalamic nuclei in frontotemporal dementia: mediodorsal nucleus involvement is universal but pulvinar atrophy is unique to C9orf72. *Hum. Brain Mapp.* 41 (4), 1006–1016. <https://doi.org/10.1002/hbm.24856>.
- Braak, H., Braak, E., 1991. Neuropathological staging of Alzheimer-related changes. *Acta Neuropathol.* 82 (4), 239–259. <https://doi.org/10.1007/BF00308809>.
- Carter, C.S., Botvinick, M.M., Cohen, J.D., 1999. The contribution of the anterior cingulate cortex to executive processes in cognition. *Rev. Neurosci.* 10 (1), 49–57. <https://doi.org/10.1515/revneuro.1999.10.1.49>.
- Jan-Feb Casals-Coll, M., Sanchez-Benavides, G., Quintana, M., Manero, R.M., Rognoni, T., Calvo, L., Palomo, R., Aranciva, F., Tamayo, F., Pena-Casanova, J., 2013. Spanish normative studies in young adults (NEURONORMA young adults project): norms for verbal fluency tests. *Neurologia* 28 (1), 33–40. <https://doi.org/10.1016/j.nrl.2012.02.010>.
- Jul Cho, H., Jeon, S., Kang, S.J., Lee, J.M., Lee, J.H., Kim, G.H., Shin, J.S., Kim, C.H., Noh, Y., Im, K., Kim, S.T., Chin, J., Seo, S.W., Na, D.L., 2013. Longitudinal changes of cortical thickness in early- versus late-onset Alzheimer's disease. *Neurobiol. Aging* 34 (7), 1921 e1929–e1921 e1915. <https://doi.org/10.1016/j.neurobiolaging.2013.01.004>.
- Contador, J., Perez-Millan, A., Tort-Merino, A., Balasa, M., Falgas, N., Olives, J., Castellvi, M., Borrego-Ecija, S., Bosch, B., Fernandez-Villullas, G., Ramos-Campoy, O., Antonell, A., Bargallo, N., Sanchez-Valle, R., Sala-Llonch, R., Llado, A., Alzheimer's Disease Neuroimaging, I., 2021. Longitudinal brain atrophy and CSF biomarkers in early-onset Alzheimer's disease. *Neuroimage Clin.* 32, 102804. <https://doi.org/10.1016/j.nicl.2021.102804>.
- Aug Coughlan, G., Laczó, J., Hort, J., Minihane, A.M., Hornberger, M., 2018. Spatial navigation deficits - overlooked cognitive marker for preclinical Alzheimer disease?. *Nat. Rev. Neurol.* 14 (8), 496–506. <https://doi.org/10.1038/s41582-018-0031-x>.
- May Craig, L.A., Hong, N.S., McDonald, R.J., 2011. Revisiting the cholinergic hypothesis in the development of Alzheimer's disease. *Neurosci. Biobehav. Rev.* 35 (6), 1397–1409. <https://doi.org/10.1016/j.neubiorev.2011.03.001>.
- Feb Dale, A.M., Fischl, B., Sereno, M.I., 1999. Cortical surface-based analysis. I. Segmentation and surface reconstruction. *Neuroimage* 9 (2), 179–194. <https://doi.org/10.1006/nimg.1998.0395>.
- Nov Eckert, U., Metzger, C.D., Buchmann, J.E., Kaufmann, J., Osoba, A., Li, M., Safron, A., Liao, W., Steiner, J., Bogerts, B., Walter, M., 2012. Preferential networks of the mediodorsal nucleus and centromedian-parafascicular complex of the thalamus—a DTI tractography study. *Hum. Brain Mapp.* 33 (11), 2627–2637. <https://doi.org/10.1002/hbm.21389>.
- Jul Erskine, D., Ding, J., Thomas, A.J., Kaganovich, A., Khundakar, A.A., Hanson, P.S., Taylor, J.P., McKeith, I.G., Attems, J., Cookson, M.R., Morris, C.M., 2018. Molecular changes in the absence of severe pathology in the pulvinar in dementia with Lewy bodies. *Mov. Disord.* 33 (6), 982–991. <https://doi.org/10.1002/mds.27333>.
- Sep 26 Fischl, B., Dale, A.M., 2000. Measuring the thickness of the human cerebral cortex from magnetic resonance images. *Proc. Natl. Acad. Sci. U. S. A.* 97 (20), 11050–11055. <https://doi.org/10.1073/pnas.200033797>.
- Folstein, M.F., Folstein, S.E., McHugh, P.R., 1975. Mini-Mental State: a practical method for grading the cognitive state of patients for clinician. *J. Psychiatry Res.* 12, 189–198. [https://doi.org/10.1016/0022-3956\(75\)90026-6](https://doi.org/10.1016/0022-3956(75)90026-6).
- Nov Forno, G., Llado, A., Hornberger, M., 2021. Going round in circles-The Papez circuit in Alzheimer's disease. *Eur. J. Neurosci.* 54 (10), 7668–7687. <https://doi.org/10.1111/ejn.15494>.
- Fredericks, C.A., Brown, J.A., Deng, J., Kramer, A., Ossenkopppele, R., Rankin, K., Kramer, J.H., Miller, B.L., Rabinovici, G.D., Seeley, W.W., 2019. Intrinsic connectivity networks in posterior cortical atrophy: a role for the pulvinar? *Neuroimage Clin.* 21, 101628. <https://doi.org/10.1016/j.nicl.2018.101628>.
- Jan Friedman, N.P., Robbins, T.W., 2022. The role of prefrontal cortex in cognitive control and executive function. *Neuropsychopharmacology* 47 (1), 72–89. <https://doi.org/10.1038/s41386-021-01132-0>.

- Mar Frisoni, G.B., Pievani, M., Testa, C., Sabatelli, F., Bresciani, L., Bonetti, M., Beltramello, A., Hayashi, K.M., Toga, A.W., Thompson, P.M., 2007. The topography of grey matter involvement in early and late onset Alzheimer's disease. *Brain* 130 (Pt 3), 720–730. <https://doi.org/10.1093/brain/awl377>.
- Jan Frisoni, G.B., Testa, C., Sabatelli, F., Beltramello, A., Soininen, H., Laakso, M.P., 2005. Structural correlates of early and late onset Alzheimer's disease: voxel based morphometric study. *J. Neurol. Neurosurg. Psychiatry* 76 (1), 112–114. <https://doi.org/10.1136/jnnp.2003.029876>.
- Jun Grober, E., Buschke, H., Crystal, H., Bang, S., Dresner, R., 1988. Screening for dementia by memory testing. *Neurology* 38 (6), 900–903. <https://doi.org/10.1212/wnl.38.6.900>.
- Oct 7 Ho, G.J., Hansen, L.A., Alford, M.F., Foster, K., Salmon, D.P., Galasko, D., Thal, L.J., Masliah, E., 2002. Age at onset is associated with disease severity in Lewy body variant and Alzheimer's disease. *Neuroreport* 13 (14), 1825–1828. <https://doi.org/10.1097/00001756-200210070-00028>.
- Sep Homman-Ludie, J., Bourne, J.A., 2019. The medial pulvinar: function, origin and association with neurodevelopmental disorders. *J. Anat.* 235 (3), 507–520. <https://doi.org/10.1111/joa.12932>.
- Oct Hornberger, M., Wong, S., Tan, R., Irish, M., Piguette, O., Kril, J., Hodges, J.R., Halliday, G., 2012. In vivo and post-mortem memory circuit integrity in frontotemporal dementia and Alzheimer's disease. *Brain* 135 (Pt 10), 3015–3025. <https://doi.org/10.1093/brain/awx239>.
- Dec Iglesias, J.E., Insausti, R., Lerma-Usabiaga, G., Bocchetta, M., Van Leemput, K., Greve, D.N., van der Kouwe, A., Alzheimer's Disease Neuroimaging, I., Fischl, B., Caballero-Gaudes, C., Paz-Alonso, P.M., 2018. A probabilistic atlas of the human thalamic nuclei combining ex vivo MRI and histology. *Neuroimage* 183, 314–326. <https://doi.org/10.1016/j.neuroimage.2018.08.012>.
- May Ilyas, A., Pizarro, D., Romeo, A.K., Riley, K.O., Pati, S., 2019. The centromedian nucleus: anatomy, physiology, and clinical implications. *J. Clin. Neurosci.* 63, 1–7. <https://doi.org/10.1016/j.jocn.2019.01.050>.
- Apr Jack Jr., C.R., Bennett, D.A., Blennow, K., Carrillo, M.C., Dunn, B., Haeberlein, S.B., Holtzman, D.M., Jagust, W., Jessen, F., Karlawish, J., Liu, E., Molinuevo, J.L., Montine, T., Phelps, C., Rankin, K.P., Rowe, C.C., Scheltens, P., Siemers, E., Snyder, H.M., Sperling, R., Contributors, 2018. NIA-AA Research Framework: toward a biological definition of Alzheimer's disease. *Alzheimers Dement* 14 (4), 535–562. <https://doi.org/10.1016/j.jalz.2018.02.018>.
- Koedam, E.L., Lauffer, V., van der Vlies, A.E., van der Flier, W.M., Scheltens, P., Pijnenburg, Y.A., 2010. Early-versus late-onset Alzheimer's disease: more than age alone. *J. Alzheimers Dis* 19 (4), 1401–1408. <https://doi.org/10.3233/JAD-2010-1337>.
- Dec Low, A., Mak, E., Malpetti, M., Chouliaras, L., Nicastro, N., Su, L., Holland, N., Rittman, T., Rodriguez, P.V., Passamonti, L., Bevan-Jones, W.R., Jones, P.S., Rowe, J.B., O'Brien, J.T., 2019. Asymmetrical atrophy of thalamic subnuclei in Alzheimer's disease and amyloid-positive mild cognitive impairment is associated with key clinical features. *Alzheimers Dement. (Amst)* 11, 690–699. <https://doi.org/10.1016/j.dadm.2019.08.001>.
- May McKhann, G.M., Knopman, D.S., Chertkow, H., Hyman, B.T., Jack Jr., C.R., Kawas, C.H., Klunk, W.E., Koroshetz, W.J., Manly, J.J., Mayeux, R., Mohs, R.C., Morris, J.C., Rossor, M.N., Scheltens, P., Carrillo, M.C., Thies, B., Weintraub, S., Phelps, C.H., 2011. The diagnosis of dementia due to Alzheimer's disease: recommendations from the National Institute on Aging-Alzheimer's Association workgroups on diagnostic guidelines for Alzheimer's disease. *Alzheimers Dement* 7 (3), 263–269. <https://doi.org/10.1016/j.jalz.2011.03.005>.
- Nov Mendez, M.F., 2012. Early-onset Alzheimer's disease: nonamnestic subtypes and type 2 AD. *Arch. Med. Res.* 43 (8), 677–685. <https://doi.org/10.1016/j.arcmed.2012.11.009>.
- Sep Murray, M.E., Graff-Radford, N.R., Ross, O.A., Petersen, R.C., Duara, R., Dickson, D.W., 2011. Neuropathologically defined subtypes of Alzheimer's disease with distinct clinical characteristics: a retrospective study. *Lancet Neurol.* 10 (9), 785–796. [https://doi.org/10.1016/S1474-4422\(11\)70156-9](https://doi.org/10.1016/S1474-4422(11)70156-9).
- Ouhaz, Z., Fleming, H., Mitchell, A.S., 2018. Cognitive functions and neurodevelopmental disorders involving the prefrontal cortex and mediodorsal thalamus. *Front. Neurosci.* 12, 33. <https://doi.org/10.3389/fnins.2018.00033>.
- Papez, J.W., 1937. A proposed mechanism of emotion. *Arch. Neurol. Psychiatr.* 38 (4), 725–743. <https://doi.org/10.1001/archneurpsyc.1937.02260220069003>.
- Pardilla-Delgado, E., Torrico-Teave, H., Sanchez, J.S., Ramirez-Gomez, L.A., Baena, A., Bocanegra, Y., Vila-Castelar, C., Fox-Fuller, J.T., Guzman-Velez, E., Martinez, J., Alvarez, S., Ochoa-Escudero, M., Lopera, F., Quiroz, Y.T., 2021. Associations between subregional thalamic volume and brain pathology in autosomal dominant Alzheimer's disease. *Brain Commun.* 3 (2), fcab101. <https://doi.org/10.1093/braincomms/fcab101>.
- Apr 15 Parnaudeau, S., Bolkan, S.S., Kellendonk, C., 2018. The mediodorsal thalamus: an essential partner of the prefrontal cortex for cognition. *Biol. Psychiatr.* 83 (8), 648–656. <https://doi.org/10.1016/j.biopsych.2017.11.008>.
- Mar Perry, J.C., Pakkenberg, B., Vann, S.D., 2019. Striking reduction in neurons and glial cells in anterior thalamic nuclei of older patients with Down syndrome. *Neurobiol. Aging* 75, 54–61. <https://doi.org/10.1016/j.neurobiolaging.2018.11.009>.
- Pintzka, C.W., Hansen, T.I., Evensmoen, H.R., Haberg, A.K., 2015. Marked effects of intracranial volume correction methods on sex differences in neuroanatomical structures: a HUNT MRI study. *Front. Neurosci.* 9, 238. <https://doi.org/10.3389/fnins.2015.00238>.
- Apr Samgard, K., Zetterberg, H., Blennow, K., Hansson, O., Minthon, L., Londo, E., 2010. Cerebrospinal fluid total tau as a marker of Alzheimer's disease intensity. *Int. J. Geriatr. Psychiatr.* 25 (4), 403–410. <https://doi.org/10.1002/gps.2353>.
- Sep 1 Scholl, M., Ossenkoppele, R., Strandberg, O., Palmqvist, S., Swedish Bio, F.S., Jogi, J., Ohlsson, T., Smith, R., Hansson, O., 2017. Distinct 18F-AV-1451 tau PET retention patterns in early- and late-onset Alzheimer's disease. *Brain* 140 (9), 2286–2294. <https://doi.org/10.1093/brain/awx171>.
- Feb Schott, J.M., Crutch, S.J., 2019. Posterior cortical atrophy. *Continuum* 25 (1), 52–75. <https://doi.org/10.1212/CON.0000000000000696>.
- Smits, L.L., Pijnenburg, Y.A., Koedam, E.L., van der Vlies, A.E., Reuling, I.E., Koene, T., Teunissen, C.E., Scheltens, P., van der Flier, W.M., 2012. Early onset Alzheimer's disease is associated with a distinct neuropsychological profile. *J. Alzheimers Dis* 30 (1), 101–108. <https://doi.org/10.3233/JAD-2012-111934>.
- Jul 1 Su, J.H., Thomas, F.T., Kasoff, W.S., Tourdias, T., Choi, E.Y., Rutt, B.K., Saranathan, M., 2019. Thalamus Optimized Multi Atlas Segmentation (THOMAS): fast, fully automated segmentation of thalamic nuclei from structural MRI. *Neuroimage* 194, 272–282. <https://doi.org/10.1016/j.neuroimage.2019.03.021>.
- Dec Swartz, R.H., Black, S.E., 2006. Anterior-medial thalamic lesions in dementia: frequent, and volume dependently associated with sudden cognitive decline. *J. Neurol. Neurosurg. Psychiatry* 77 (12), 1307–1312. <https://doi.org/10.1136/jnnp.2006.091561>.
- Spring Taber, K.H., Wen, C., Khan, A., Hurley, R.A., 2004. The limbic thalamus. *J. Neuropsychiatry Clin. Neurosci.* 16 (2), 127–132. <https://doi.org/10.1176/jnp.16.2.127>.
- Tak, K., Lee, S., Choi, E., Suh, S.W., Oh, D.J., Moon, W., Kim, H.S., Byun, S., Bae, J.B., Han, J.W., Kim, J.H., Kim, K.W., 2020. Magnetic resonance imaging texture of medial pulvinar in dementia with Lewy bodies. *Dement. Geriatr. Cognit. Disord.* 49 (1), 8–15. <https://doi.org/10.1159/000506798>.
- Jul-Aug Tamayo, F., Casals-Coll, M., Sanchez-Benavides, G., Quintana, M., Manero, R.M., Rognoni, T., Calvo, L., Palomo, R., Aranciva, F., Pena-Casanova, J., 2012. [Spanish normative studies in a young adult population (NEURONORMA young adults Project): norms for the verbal span, visuospatial span, Letter-Number Sequencing, Trail Making Test and Symbol Digit Modalities Test]. *Neurologia* 27 (6), 319–329. <https://doi.org/10.1016/j.nrl.2011.12.020> (Estudios normativos españoles en población adulta joven (Proyecto NEURONORMA jóvenes): normas para las pruebas span verbal, span visuoespacial, Letter-Number Sequencing, Trail Making Test y Symbol Digit Modalities Test.).
- Apr Thomas, G.E.C., Leyland, L.A., Schrag, A.E., Lees, A.J., Acosta-Cabronero, J., Weil, R.S., 2020. Brain iron deposition is linked with cognitive severity in Parkinson's disease. *J. Neurol. Neurosurg. Psychiatry* 91 (4), 418–425. <https://doi.org/10.1136/jnnp-2019-322042>.
- Dec Tort-Merino, A., Falgas, N., Allen, I.E., Balasa, M., Olives, J., Contador, J., Castellvi, M., Junca-Parella, J., Guillen, N., Borrego-Ecija, S., Bosch, B., Fernandez-Villullas, G., Ramos-Campoy, O., Antonell, A., Rami, L., Sanchez-Valle, R., Llado, A., 2022. Early-onset Alzheimer's disease shows a distinct neuropsychological profile and more aggressive trajectories of cognitive decline than late-onset. *Ann. Clin. Transl. Neurol.* 9 (12), 1962–1973. <https://doi.org/10.1002/acn3.51689>.
- Umapathy, L., Keerthivasan, M.B., Zahr, N.M., Bilgin, A., Saranathan, M., 2021. A Contrast Synthesized Thalamic Nuclei Segmentation Scheme Using Convolutional Neural Networks. *NEUROINFORMATICS*.
- Warrington, E.K., James, M., 1991. *The Visual Object and Space Battery Perception*. Bury St Edmunds. Thames Valley Company.